Iranian Polymer Journal
https://doi.org/10.1007/s13726-026-01608-0

ORIGINAL RESEARCH

Development and optimization of a single-component moisture-curable sealant with enhanced mechanical and rheological properties

Mohaddeseh Masoudi[1] · Gholam Hossein Zohuri[1] · Omid Jawhid[2] · Mohammad Nourmohammadi[2] · Zahra Pourakbar[2]

Received: 16 April 2025 / Accepted: 15 November 2025

Abstract

This study presents a novel single-component, moisture-curable sealant formulation based on silyl-terminated polyether (MS) polymer, reinforced with synergistic nanofillers including fumed silica and nano-calcium carbonate. The primary objective was to enhance the mechanical performance, thermal stability, and rheological behavior of the MS-based system through the strategic use of nanotechnology. The optimized formulation exhibited a tensile strength of 1.73 MPa and elongation-at-break of 175%, while shear strength increased to 1.97 MPa after seven days of curing under controlled temperature and humidity. Fourier transform infrared spectroscopy (FTIR) confirmed stronger intermolecular interactions and improved crosslinking density due to the presence of reactive nanoparticles. Thermogravimetric analysis (TGA) showed a noticeable enhancement in thermal resistance, particularly with fumed silica loading up to 0.9 wt%, which delayed thermal decomposition. Additionally, nano-calcium carbonate at 31.7 wt% contributed to better dimensional stability and homogeneous filler dispersion within the polymer matrix. The inclusion of 0.6 wt% fumed silica resulted in a 155% increase in adhesive strength compared to the unfilled formulation. Rheological analysis revealed superior thixotropy and sag resistance, making the sealant suitable for precision applications such as vertical joints or overhead installations. Overall, this work underscores the potential of nanofiller-enhanced MS polymers to meet demanding performance criteria, offering a scalable and robust solution for industrial sealing applications.

Graphical abstract

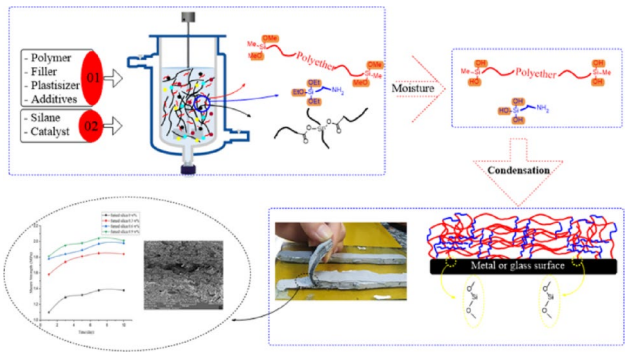

Keywords Silyl-terminated polyether · Moisture-curable sealant · Fumed silica · Nano-calcium carbonate · Rheological and thermal enhancement

✉ Gholam Hossein Zohuri
zohuri@um.ac.ir

[1] Department of Chemistry, Faculty of Science, Ferdowsi University of Mashhad, Mashhad, Iran

[2] Department of Research and Development, Ayegh Khodro Toos (AKT) Co. of Part Lastic Industry Group, P.O. Box 91851-77209, Mashhad, Iran

Published online: 12 February 2026

Introduction

Adhesive bonding technology is widely used and is an important method for connecting structures in various industries [1]. Additives, especially nanoparticles, can affect the strength of any adhesive bond, but unfortunately, quantitative research and experimental data in this area are lacking [2, 3]. Adhesive joints in engineering structures are subjected to both tensile and shear loads, so it is important to study the effect of variables such as nanomaterials and temperature on their strength under complex stress conditions [4, 5]. Previous studies have shown that the tensile strength of adhesive joints decreases with increasing temperature, and the correlation between tensile and shear properties varies in terms of stiffness, strength, and ductility of the joint [6–8]. The effect of nanoparticles on the strength of an adhesively bonded joint has been studied for specific adhesives, such as epoxy [9, 10] and polyurethane [11], with different temperature ranges and failure criteria [12]. Further research, of course, is needed to determine if these conclusions apply to other types of adhesives [13]. Silyl-modified polymer sealants also referred to as SMPs or MS polymers, have become increasingly popular in a wide range of industrial applications due to their excellent properties and versatility. These sealants are unique due to their polyether backbone which is terminated by silane groups. This structure gives them the ability to be both adhesive and sealant, making them ideal for applications requiring strong bonding and sealing properties [14]. The silane groups in the polymer backbone allow for excellent adhesion to a variety of substrates, including metals, plastics, glass, and even damp or oily surfaces [14, 15]. One of the key advantages of silyl-modified polymer sealants is their high elasticity and flexibility [16, 17]. This makes them ideal for applications where movement and vibration are common, such as in the automotive and transportation industries. Their ability to withstand extreme temperatures and weather conditions has made them a popular choice in construction and outdoor applications. In addition to their excellent physical properties, silyl-modified polymer sealants are also known for their environmentally friendly nature [18]. They are solvent-free and have low emissions, making them a preferred choice for green building projects and eco-conscious industries. SMPs also are an alternative to polyurethanes, as they do not have unreacted isocyanate groups and have additional benefits such as lower static charge, no shrinkage after curing, and paint ability. In this context, recent research on the curing kinetics and structure–property relationship of moisture-cured one-component polyurethane adhesives has provided valuable insights into the performance and reliability of such systems [19].

The present study involved the preparation of a moisture-curing sealant incorporating silica nanoparticles. The thermal and mechanical properties of the sealant were investigated before and after adding the nano-additive. The insights derived from this work establish a paradigm for designing high-performance materials with tailored mechanical resilience, thermal stability, and adhesive capabilities. These findings not only address pressing industrial demands but also inspire future innovations across diverse sectors, underscoring the transformative potential of nanoscale engineering in polymer chemistry.

Experimental

Materials

The silyl-terminated polymer (S303H, viscosity 10000–15000 cP, moisture: ≤ 0.1 wt%, pH 6.0–8.0) was acquired from Kaneka Co. Japan. (3-Aminopropyl) triethoxysilane (APTES) was supplied from Sigma Aldrich Co. USA. Dibutyltin dilaurate (DBTDL) was obtained from Rezitan Co. Iran. Nano-calcium carbonate (OMYA CARB 5-SW) was obtained from Omya Pars Co. Iran. Anti-oxidant (SONGNOX 1680) was purchased from Songwon Industrial Co. LTD, Korea. Anti-UV (Tinuvin 326) from Ciba Specialty Chemicals Co. Switzerland, titanium dioxide (Crimea Tiox 280), fumed silica (Aerosil 200, specific surface area (BET): 175–225 m^2/g, SiO_2 content: >99.8%, tamped density: approx. 50 g/L), and diisononyl phthalate (DINP) were all commercially available in industrial grade. All the aforementioned materials and reagents were utilized directly without any additional purification.

Preparation of sealant

The filler materials (minerals) were dehydrated (at 120 °C for 24 h) before use. Compounding of the materials was carried out using a double-plate mixing tank. The preparation of blank compound (without a nano-additive) followed by: silyl-terminated polyether polymer (33.5 wt%) which was masticated by using slowly adding nano-calcium carbonate (31.7 wt%) and then diisononyl phthalate (15 wt%), titanium dioxide (15.8 wt%), moisture absorbent based on aluminum silicate (0.5 wt%), anti-oxidant (0.71 wt%), anti-UV (0.71 wt%) were added and mixed (2 h under vacuum, 120 °C, 205 rpm). The produced master batch was cooled to room temperature (< 40 °C), followed by adding APTES (1.5 w%), and DBTDL (0.5 wt%), and mixing under inert conditions (10 min) to prepare the final mastic adhesive. Finally, the product was packed under an inert gas. Preferably, the humidity level is 1000–2000 ppm.

Table 1 Effect of fumed silica on the viscosity of the sealant

Fumed silica (wt%)	Viscosity	Flow
0	1.18×10^7 mPa.s	Sagging: 1 mm
0.3	1.42×10^7 mPa.s	No sagging
0.6	2.16×10^7 mPa.s	No sagging
0.9	3.13×10^7 mPa.s	No sagging

Table 2 Effect of the fumed silica on the peeling strength of the samples

Fumed silica	T-peeling on metal (kg.f/25 mm)	T-Peeling on glass
0%	17.8	70% CF
0.3%	19.3	Min. 99% CF
0.6%	21.8	Min. 99% CF
0.9%	20.3	Min. 99% CF

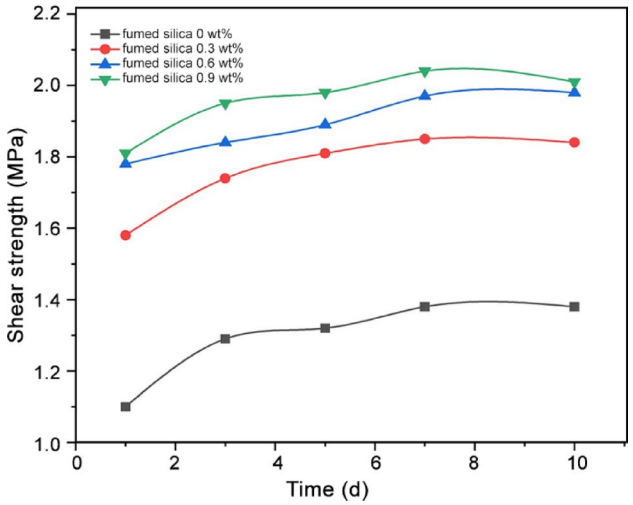

Fig. 1 Effect of the fumed silica concentration and curing time on the shear strength of the sealant

To improve adhesion and investigate the effect of the fumed silica on the mechanical properties of the MS sealant, different percentages of the fumed silica (0.3, 0.6, and 0.9 wt%) were added to the formula and compared with the series without the fumed silica.

Characterization

The sealants were cured in standard conditions (23 ± 2 °C and relative humidity of 50 ± 5%) for 1 to 10 days. The mechanical properties of the samples were measured via a mechanical testing system (Santam STM-5) operating at 50 mm/min tensile speed (ASTM D 451545, 2006). The viscosity and thixotropy (according to DIN SPEC 91143-2) of the sealant samples were measured (at 25 °C) using a rotational rheometer (Anton Paar, ViscoTherm VT2 model) in steady shear mode, equipped with spindle CC10. The hardness of the samples (T = 6 mm) was measured using a Shore A durometer (Santam SHD-05, ASTM D2240). The hardness was read within 30 s of firm contact with the specimen. T-peeling strength study was performed on a glass plate before and after aging, so that the samples were peeled at an angle of 90 degrees every 5 mm (ASTM D 511709, 2005). Chemical structure of the materials followed by using FTIR spectroscopy (Thermo-Nicolet Avatar 370) using a standard KBr pellet technique. Thermogravimetric analysis (Mettier Toledo-TGA, Switzerland) was conducted to mass loss percentage measuring of the products, (heating rate of 10 °C/min from 25 to 800 °C) under an argon atmosphere.

Results and discussion

Effect of additive on viscosity

The viscosity of the final compound increases with the rising concentration of fumed silica, as shown in Table 1. This behavior is primarily attributed to the incorporation of fumed silica particles within the free volume of the polymer matrix. The presence of these nanoparticles restricts the mobility of polymer chains, resulting in increased intermolecular interactions and, consequently, a notable rise in viscosity (Table 2).

Shear strength

The full strength of the prepared sealant may take several days to develop. Thus, the strength measurement was carried out after 1, 3, 5, 7, and 10 days of surface drying of the products (Fig. 1). The shear strength has raised with increasing of the fumed silica concentration. This increase can be attributed to the sufficient chemical interaction between the additive and the components of the sealant composition due to the formation of a three-dimensional network [14]. The adhesion strength of the sealant composition was raised with the increasing percentage of the fumed silica, which could be because of hydrogen interactions with the sealant matrix. Also, the shear strength of the products was increased with drying time, so that the shear strength reached its maximum value (1.97 MPa, after 7 days) using 0.6 wt% of the fumed silica. This value is 2.6 times higher than the original sealant. However, longer curing times (up to 10 days) had little effect on shear strength (Fig. 1).

Tensile strength and elongation-at-break

Incorporation of the fumed silica (up to 0.6 wt%) resulted in enhancement of the tensile strength (from 1.15 to 1.73 MPa), while, elongation at break was reduced (from 233 to 175). The reason can probably be related to the high strength of the fumed silica and its favorable distribution in

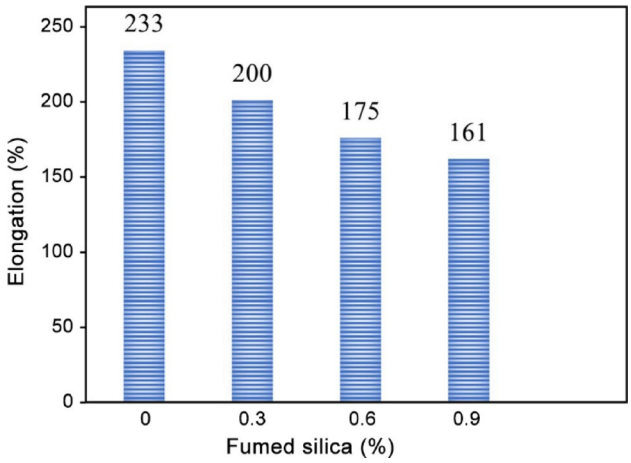

Fig. 2 Effect of the fumed silica concentration on elongation-at-break of the sealant

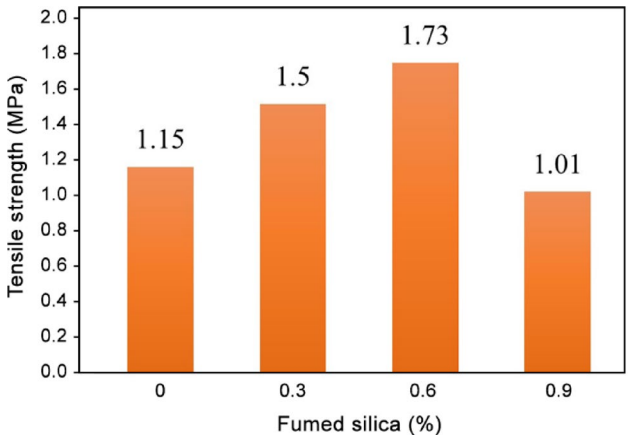

Fig. 3 Effect of the fumed silica concentration on the tensile strength of the sealant

the field of resin [20]. The introduction of additional fumed silica (0.9 wt%) resulted in an abrupt decline in the tensile strength. This phenomenon is believed to be attributed to the agglomeration of the silica particles, leading to the formation of multiple regions within the sealant matrix that are prone to crack formation (Figs. 2 and 3).

T-Peeling strength

As shown in Fig. 4a, the neat (blank) sealant exhibited poor adhesion to the metal surface, with clear interfacial failure zones where the sealant was entirely detached from the substrate (marked areas). This behavior is attributed to the lack of reinforcement and insufficient interaction at the polymer-metal interface, leading to adhesive failure. In contrast, the incorporation of fumed silica at 0.6 wt% (Fig. 4c) improved the interfacial bonding, evidenced by cohesive failure patterns indicating stronger matrix-substrate interactions. However, increasing the fumed silica content to 0.9 wt% (Fig. 4d) resulted in a decline in peel strength, with similar adhesive failure zones reappearing (circled areas). This performance reduction is likely due to the aggregation of nanoparticles and their poor dispersion, which disrupts the matrix homogeneity and weakens the filler-polymer and filler-substrate interactions. These observations emphasize the critical role of uniform nanoparticle dispersion in enhancing adhesion strength. On the glass substrate (Fig. 4e and f), the peeling behavior revealed mainly cohesive failure across all samples, highlighting good compatibility and interaction between the sealant and glass surface.

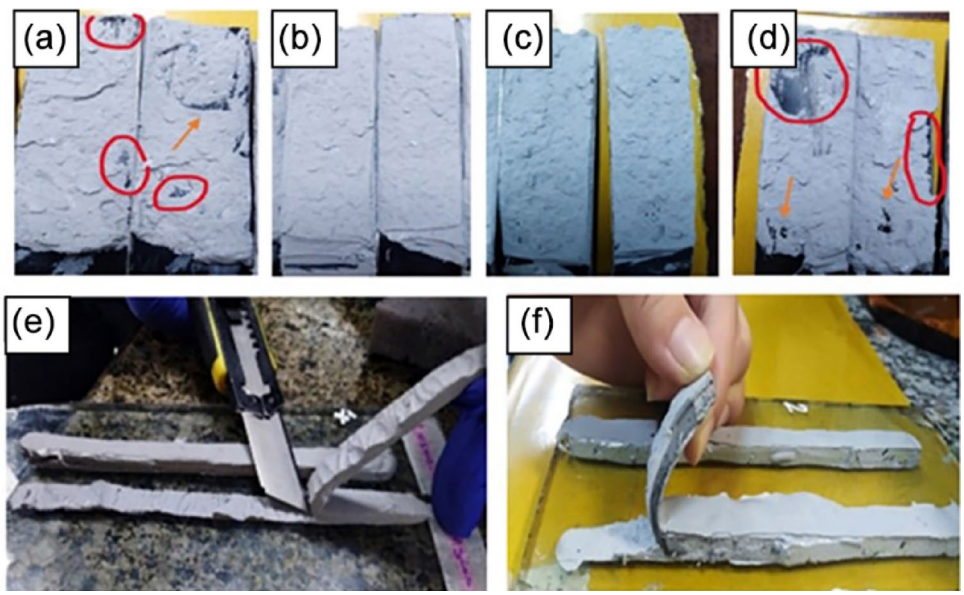

Fig. 4 T-Peeling tests of the samples on metal: **a** blank sample, **b** fumed silica 0.3 wt%, **c** fumed silica 0.6 wt%, **d** fumed silica 0.9 wt%, and **e** and **f** T-peeling tests of the samples on glass

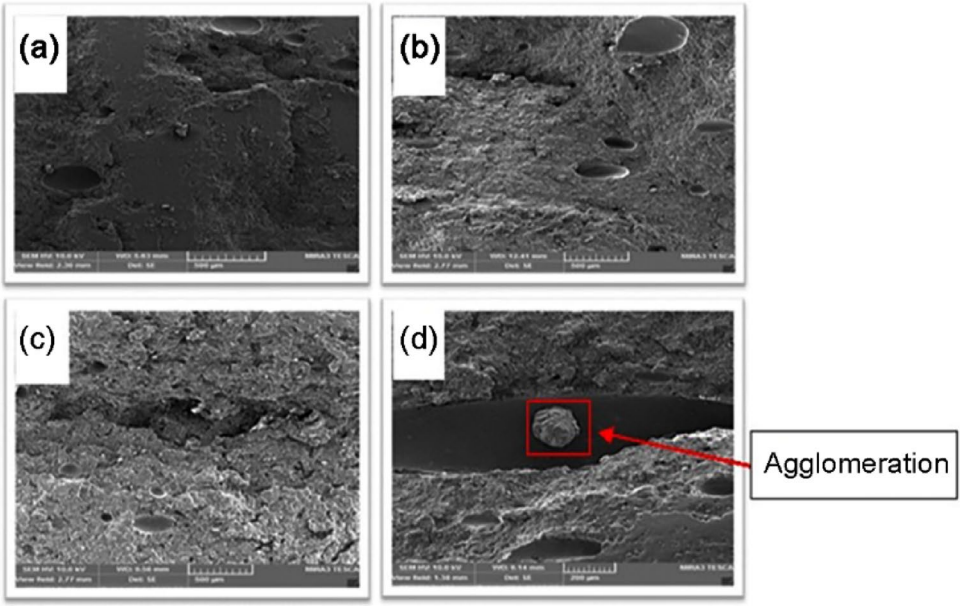

Fig. 5 FE-SEM image of the samples: **a** blank sample, **b** fumed silica 0.6 wt%, **c** fumed silica 0.9 wt%, and **d** agglomeration of the fumed silica

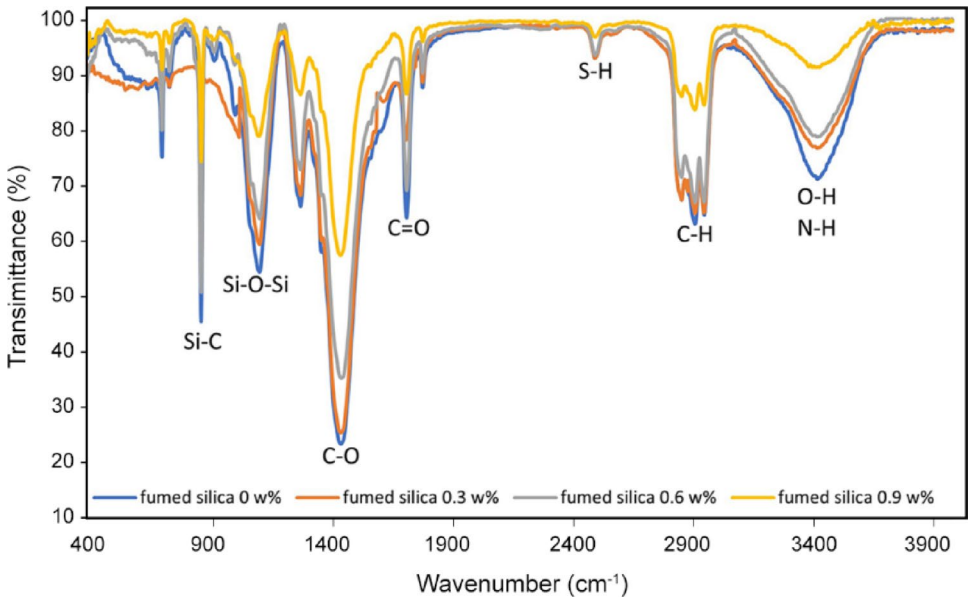

Fig. 6 FTIR of the produced blank sample and nanoparticles containing samples

Morphological study

By comparing the images of the fracture surfaces involved in the blank sample and the sealant (containing 0.6 and 0.9 wt% of the fumed silica), it can be seen that the presence of fumed silica has led to the change of the smooth fracture surface to a far more wavy and uneven fracture surface in the sealants containing 0.6 wt% (Fig. 5), which requires more energy to fail. The FE-SEM image of the fracture surface of sealants containing 0.9 wt% fumed silica shows that agglomerated areas have been created (Fig. 5d), and these factors have led to a decrease in the fracture energy of the sealant compared to the sealant containing 0.6 wt%.

Structural study

FTIR results of MS sealant with different weight percentages were studied (Fig. 6). The most important characteristic peaks in the FTIR spectra are as follows: the broad spectrum around the wavelength of 3400 cm^{-1} is related to the stretching vibration of both (O-H) and (N-H) functional groups of MS polymer and APTES, respectively. The peak at 2967, 2928, and 2871 cm^{-1} indicates the stretching vibration of (C-H) in polyether resin. The peak at 1729, 1455 and 1371 cm^{-1} are respectively in the range of stretching vibration corresponding to the (C=O) functional group of DINP, CH_2, and CH_3, and the peak at 2508 cm^{-1} can correspond to Si-H stretching modes. The results show that no

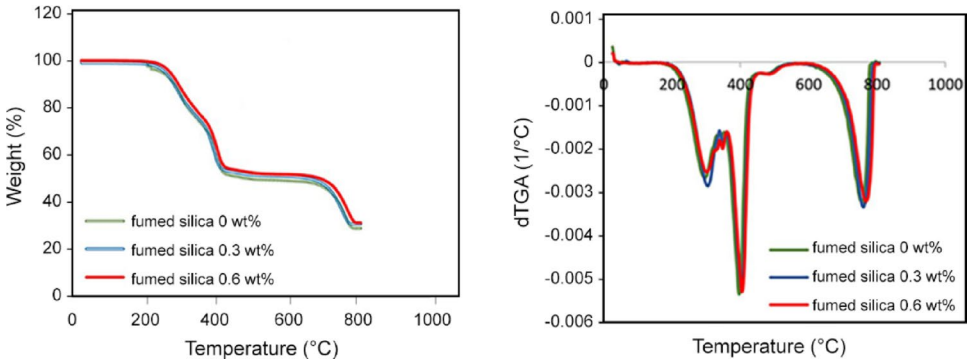

Fig. 7 TGA and DTG curves of the MS sealants

new peaks were created in the FTIR spectrum by adding the fumed silica, and none of the peaks were removed. The most important point of this phenomenon can be attributed to the so low percentage of fumed silica reinforcement in the sealant. A comparison of the FTIR study on the transformation of MS raw sealant and the fumed silica shows that the peak related to O–H stretching vibration is slightly wider in the sample containing the fumed silica, while, the intensity of the peak decreases compared to the sample without of the fumed silica. This occurrence signifies the involvement of the hydroxyl functional group in establishing a link between the connection field and the reinforcement within the nanocomposite.

Thermal gravimetric analysis (TGA)

The thermal stability of the sealant samples containing 0, 0.3, and 0.6 wt% fumed silica was evaluated using thermogravimetric analysis (TGA). The samples were heated from room temperature to 800 °C at a constant rate of 10 °C/min under an argon atmosphere (as illustrated in Fig. 7). The onset temperature was determined at 5 wt% mass loss. The decomposition process occurred in three distinct stages. The initial stage of mass loss, observed around 200 °C, precedes the main degradation event and is primarily attributed to the evaporation of small molecules such as softening agents, water, and the degradation of secondary hydroxyl groups. In the samples containing 0.3 and 0.6 wt% fumed silica, this initial mass loss occurred at higher temperatures, suggesting restricted molecular mobility. This behavior can be explained by hydrogen bonding between the silyl-functionalized polyether chains and the hydroxyl groups present on the surface of the silica particles, which contributes to the formation of a three-dimensional network that hinders the release of small molecules. The second stage, around 400 °C, is marked by a sharp decline in mass, corresponding to the thermal degradation of the polyether backbone. The final stage involves the breakdown of more thermally stable components such as carbon black and inorganic fillers.

Table 3 Thermal stability indices of the MS sealants

Fumed silica	Degradation onset temperature (°C)	Maximum destruction temperature (°C)	Amount of residual coal (%)
0%	196	398	31.49
0.3%	200	400	31.95
0.6%	208	404	32.10

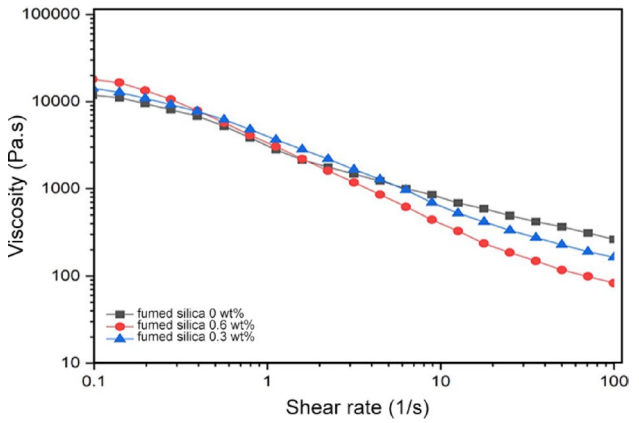

Fig. 8 Effect of the fumed silica concentration on the rheological of the sealants

Notably, the sample with 0.6 wt% fumed silica exhibited a slightly higher residual mass compared to the neat sample, which is attributed to the increased content of inorganic silica filler. A detailed summary of thermal stability parameters for the MS sealants with varying fumed silica concentrations is presented in Table 3.

Rheological properties

Fumed silica is widely recognized as an effective rheology modifier in sealant formulations, primarily used to control flow behavior and enhance thixotropy. The viscosity of the formulated sealants was measured using a rheometer, as illustrated in Fig. 8. Results indicate that increasing the weight% of fumed silica leads to a more pronounced decrease in viscosity with increasing shear rate. This

shear-thinning behavior becomes more evident with higher fumed silica content, reflecting improved thixotropic characteristics and enhanced flowability. These features are particularly advantageous during sealant application, as they facilitate easier injection and handling.

Figure 9 shows the evolution of viscosity in adhesives containing different amounts of fumed silica. At the beginning, all systems display relatively high viscosity, which is related to the existence of a stable network structure in the matrix. When shear is applied, the viscosity drops sharply as physical interactions are disrupted and the three-dimensional particle-polymer network is broken down. This reduction improves the flowability of the adhesive and facilitates its application. After removing the shear, the recovery of viscosity was monitored. The reference sample without nanoparticles was unable to rebuild its structure, and the viscosity remained at a lower level. With a small amount of fumed silica, partial recovery was observed, although the initial state was not completely restored. At higher loadings, however, the viscosity almost returned to the original value. This suggests that larger specific surface area and stronger particle-matrix interactions at higher silica content facilitate faster network reconstruction. Overall, increasing the concentration of fumed silica strengthens the thixotropic response, allowing the adhesive to remain injectable while regaining rheological stability after shear.

Considering the optimized properties of the adhesive, including high viscosity, appropriate thixotropic behavior, acceptable shear and tensile strength, thermal stability, and compatibility with both metallic and glass substrates, this formulation is particularly suitable for applications such as glass installation and sealing, vertical and overhead joints in the construction industry, as well as general sealing purposes under variable climatic conditions. Its ease of application, one-component nature, and reliable mechanical performance make this system a promising alternative to more complex two-component adhesives.

Conclusion

The fumed silica in the sealant composition plays a crucial role in its mechanical properties. The viscosity, shear strength, adhesion strength, and tensile strength are influenced by the addition of the fumed silica. Increasing the concentration of the fumed silica leads to an increase in all behaviors. Higher concentrations of fumed silica, however, result in a lower percentage of elongation, indicating a more rigid and less flexible sealant. Beyond a certain concentration, typically around 0.6 wt%, the peel strength of the sealant may start to decrease. The formation of a three-dimensional network, facilitated by the presence of the fumed silica, hinders the release of small molecules during thermal degradation. This leads to improved thermal stability and resistance to degradation, making the sealant more durable and long-lasting. With the increase of the fumed silica, the shear strength increased with time, and after 7 days, the shear strength reached its maximum value (1.97 MPa). Tensile strength and elongation percentage improved up to 0.6 wt% of the fumed silica and reached 1.54 MPa and 165%, respectively. The rheological properties were improved, so that with increasing fumed silica, the initial viscosity increased, which prevented the sealant from sagging during application, with the rise of the shear rate, the viscosity further decreased and thixotropy was improved, which could help the injection of the sealant during application. The shear strength in the sample containing 0.6 wt% of the fumed silica reached 21.8 kg. /mm, which has improved by 22.47% compared to the sample without the fumed silica. The thermal resistance of the sealant modified with the fumed silica (0.6 wt%) had a slightly higher start temperature and maximum degradation temperature than the sample without the fumed silica and other modified samples.

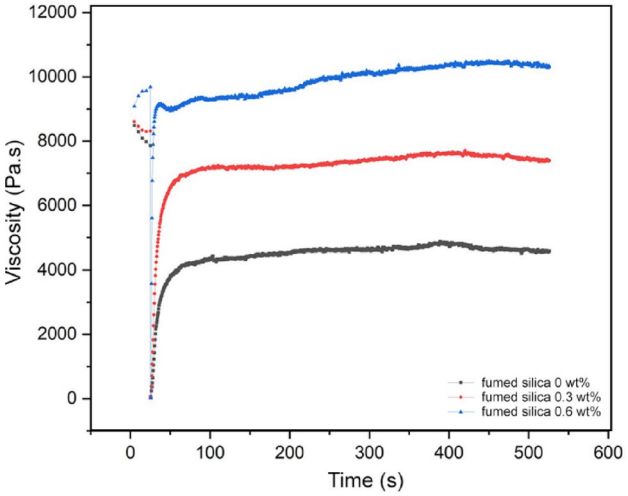

Fig. 9 Effect of the fumed silica concentration on the thixotropic of the sealants

Author contributions All authors were involved in the conception and design of the study. The preparation of materials, the initial draft of the manuscript, as well as the collection and analysis of data, were carried out by Mohaddeseh Masoudi and Omid Jawhid. Professor Gholam Hossein Zohuri supervised and edited the manuscript. Ultimately, Mohammad Nourmohammadi, and Zahra Pourakbar reviewed and approved the final version of the manuscript.

Funding This research initiative received funding from Ferdowsi University of Mashhad, located in Mashhad, Iran (Grant numbers [3/56597]), along with technical and chemical assistance provided by Ayegh Khodro Toos (AKT) Co., a member of the Part Lastic Industrial Group in Iran.

Declarations

Conflict of interest The authors declare no conflict of interest.

References

1. Ehrhart B, Valeske B, Bockenheimer C (2013) Non-destructive evaluation (NDE) of aerospace composites: methods for testing adhesively bonded composites, 1st edn. Elsevier, Arlington
2. Akpinar IA, Gultekin K, Akpinar S, Akbulut H, Ozel A (2017) Research on strength of nanocomposite adhesively bonded composite joints. Compos Part B 126:143–152. https://doi.org/10.1016/j.compositesb.2017.06.016
3. Srivatsa JT, Ziaja MB (2011) An experimental investigation on use of nanoparticles as fluid loss additives in a surfactant-polymer based drilling fluids. Int Petroleum Technol Conf (IPTC). https://doi.org/10.2523/IPTC-14952-MS
4. Anaç N, Doğan Z (2023) The effect of organic fillers on the mechanical strength of the joint in the adhesive bonding. Processes 11:406. https://doi.org/10.3390/pr11020406
5. Uttaravalli AN, Dinda S, Bethi B, Praveen BVS, Gidla BR (2022) Use of additives to improve bonding strength of the adhesive prepared from used polymer: sustainable management approach. Mater Today 59:120–127. https://doi.org/10.1016/j.matpr.2021.10.269
6. Na J, Mu W, Qin G, Tan W, Pu L (2018) Effect of temperature on the mechanical properties of adhesively bonded basalt FRP-aluminum alloy joints in the automotive industry. Int J Adhes Adhes 85:138–148. https://doi.org/10.1016/j.ijadhadh.2018.05.027
7. Banea M, Da Silva LF, Carbas R, De Barros S (2018) Effect of temperature and moisture on the tensile properties of a TEPs-modified adhesive. Mater Plast 55:478–481. https://doi.org/10.37358/MP.18.4.5057
8. Banea MD, De Sousa FSM, Da Silva LFM, Campilho RDSG, De Pereira AB (2011) Effects of temperature and loading rate on the mechanical properties of a high temperature epoxy adhesive. J Adhes Sci Technol 25:2461–2474. https://doi.org/10.1163/016942411X580144
9. Saraç İ, Adin H, Temiz Ş (2019) Investigation of the effect of use of Nano-Al_2O_3, Nano-TiO_2 and nano-SiO_2 powders on strength of single lap joints bonded with epoxy adhesive. Compos Part B 166:472–482. https://doi.org/10.1016/j.compositesb.2019.02.007
10. Zhai LL, Ling GP, Wang YW (2008) Effect of nano-Al_2O_3 on adhesion strength of epoxy adhesive and steel. Int J Adhes Adhes 28:23–28. https://doi.org/10.1016/j.ijadhadh.2007.03.005
11. Rodríguez R, Pérez B, Flórez S (2014) Effect of different nanoparticles on mechanical properties and curing behavior of thermoset polyurethane adhesives. J Adhes 90:848–859. https://doi.org/10.1080/00218464.2014.893509
12. Çetin ME (2022) Investigation of carbon nanotube reinforcement to polyurethane adhesive for improving impact performance of carbon fiber composite sandwich panels. Int J Adhes Adhes 112:103002. https://doi.org/10.1016/j.ijadhadh.2021.103002
13. Tian Y, Huang X, Cheng Y, Niu Y, Ma J, Zhao Y, Kou X, Ke Q (2022) Applications of adhesives in textiles: a review. Eur Polym J 167:111089. https://doi.org/10.1016/j.eurpolymj.2022.111089
14. Guillaume SM (2018) Advances in the synthesis of silyl-modified polymers (SMPs). Polym Chem 9:1911–1926
15. Nečasová B, Kovářová B, Liška P, Šlanhof J (2015) Determination of adhesion of Silyl modified polymer adhesives to wooden façade cladding–case study. Procedia Eng 108:410–418. https://doi.org/10.1016/j.proeng.2015.06.165
16. Na J, Liu Y, Fan Y, Mu W, Chen X, Yan Y (2017) Effect of temperature on the joint strength of a silyl-modified polymer-based adhesive. J Adhes 93:626–639. https://doi.org/10.1080/00218464.2015.1128330
17. Kim YJ, Hyun SW, Yoshitake I, Kang JY (2014) Residual performance of a silyl-modified polymer adhesive for CFRP-steel interface exposed to thermally-induced stress States. Int J Adhes Adhes 51:117–127. https://doi.org/10.1016/j.ijadhadh.2014.03.003
18. Pape PG (2011) Applied plastics engineering handbook, 2nd edn. Elsevier (William Andrew Publishing)
19. Hojun M, Jeong EP, Woongbi C, Jaecheol J, Jeong JW (2023) Curing kinetics and structure-property relationship of moisture-cured one-component polyurethane adhesives. Eur Polym J 201:112579. https://doi.org/10.1016/j.eurpolymj.2023.112579
20. Abenojar J, Tutor J, Ballesteros Y, Del Real JC, Martínez MA (2017) Erosion-wear, mechanical and thermal properties of silica filled epoxy nanocomposites. Compos Part B 120:42–53. https://doi.org/10.1016/j.compositesb.2017.03.047